Relativistic Heavy Ion Collisions and String Theory

Josh Friess
Princeton University

in collaboration with Steve Gubser, Georgios Michalogiorgakis, and Silviu Pufu

KITP String Phenomenology 2006

1. Introduction

The Relativistic Heavy Ion Collider (RHIC), operating at Brookhaven National Laboratory, collides gold on gold.

- Total center of mass energy is about $39\,\mathrm{TeV}$.
- There is good evidence that a thermalized quark-gluon plasma (QGP) forms with temperature above the confinement scale, $T_C \approx 170\mathrm{MeV} \approx 2 \times 10^{12} K$

The theoretical understanding of RHIC physics is imperfect.

- The QGP is strongly coupled, so perturbative QCD is of limited utility.
- Lattice calculations provide good information about static properties, e.g., T_C for confinement, but not transport properties (like viscosity).
- String theory, in particular AdS/CFT, offers an alternative description of strongly coupled gauge theory.

Two main themes of the AdS/CFT - RHIC connection are

A The viscosity bound $\eta/s \geq \hbar/4\pi$.

B Jet-quenching and the drag force on hard partons, especially heavy quarks.

A has been under discussion for about 5 years. B is a relatively new development, and the focus of our contribution.

2. What happens at RHIC?

RHIC accelerates beams of heavy nuclei (gold, copper, etc.) in opposite directions around a large circular ring and collides them.

Gold nuclei are nearly spherical with radius of about $7\,\mathrm{fm}$ in rest frame; Lorentz contraction reduces front-to-back length to $\sim 0.07\mathrm{fm}$.

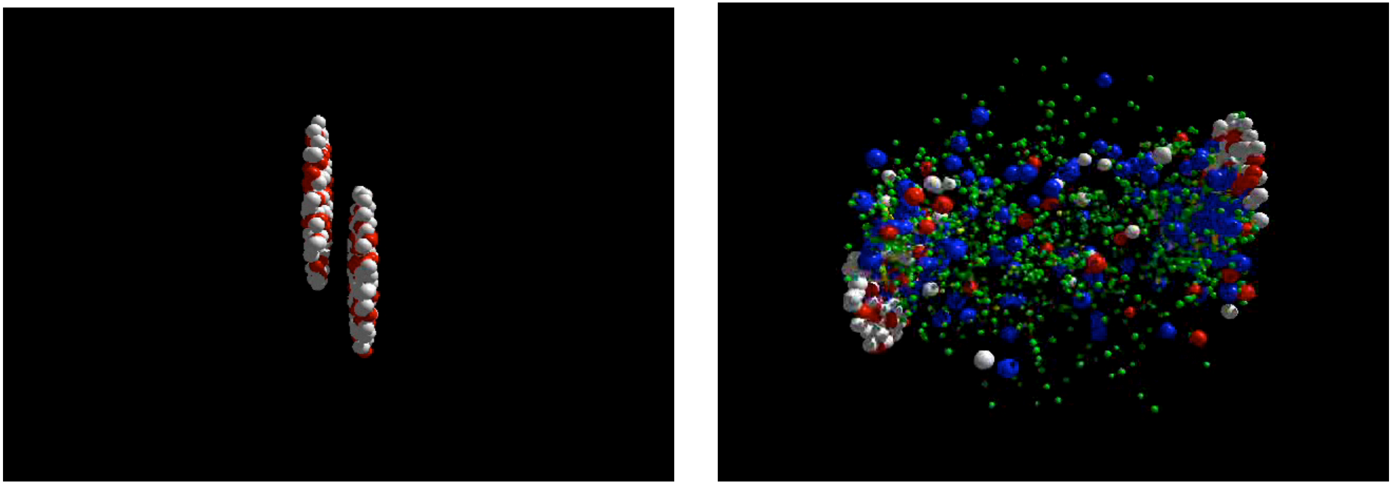

Figure 1: *Before-and-After shots of ultra-relativistic dynamics simulation of a gold-gold collision [1].*

- The main ring is $3.8\,\mathrm{km}$ in circumference.
- Beam CM energy per nucleon per nucleon is $\sqrt{s_{NN}} = 200\,\mathrm{GeV}$.
- RHIC's design luminosity is $2 \times 10^{26}\,\mathrm{cm}^{-2}\mathrm{s}^{-1}$. Integrated luminosity to date is in the ballpark of $4\,\mathrm{nb}^{-1}$.

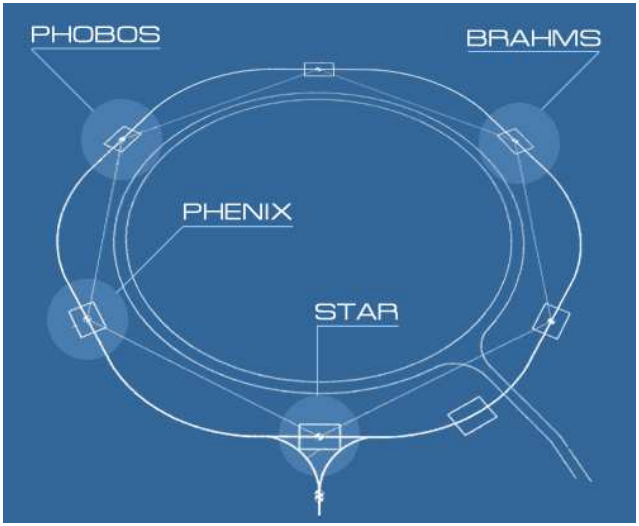

Experimentalists claim that a thermalized QGP gets formed. Hadron yields follow nearly Boltzmann distributions (Kaneta 2004 [2]):

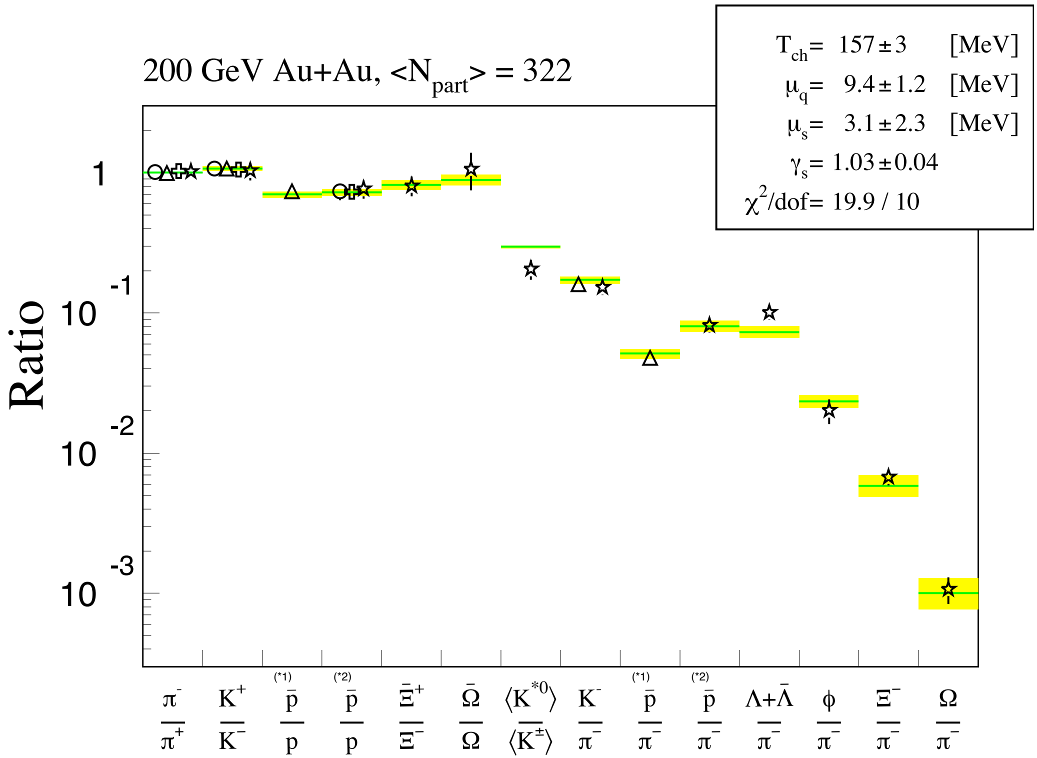

Figure 2: *Yellow lines are thermal model predictions, icons represent experimental data. T_{ch} is chemical freeze-out temperature, μ_q is up/down chemical potential, μ_s is strange chemical potential, and γ_s is strangeness saturation.*

Furthermore, theoretical predictions from lattice simulations find that deconfinement happens at $T_c \approx 170\,\mathrm{MeV}$, and that ϵ/T^4 has a plateau at 80% of the free field value (Karsch 2001 [3]):

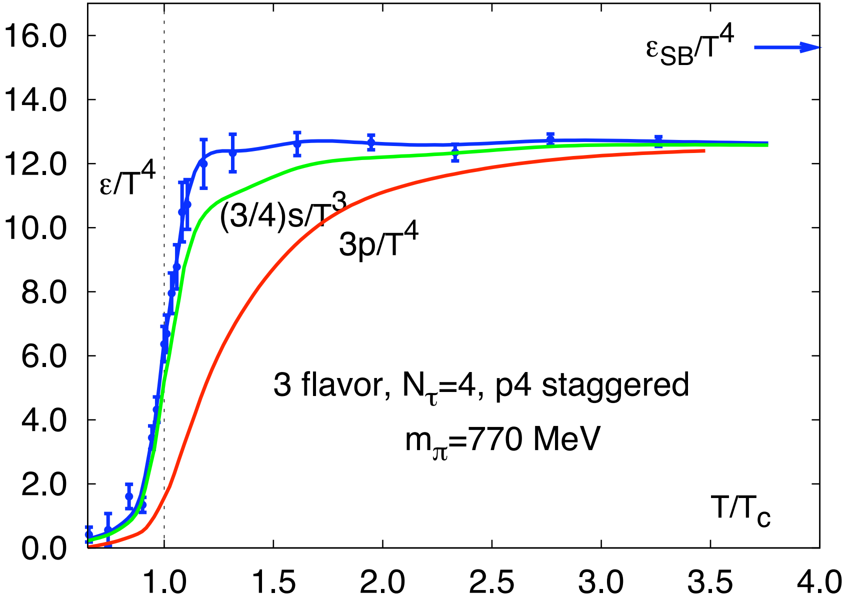

Figure 3: *Lattice results for the equation of state of QCD.*

Jet-quenching refers to the rapid loss of energy of a hard parton propagating through the hot dense matter created in a gold-gold collision. The prima facie evidence for jet quenching is the the suppression of high p_T jets (more precisely, high p_T hadrons) relative to expectations from “binary collsion scaling.”

- Jet production from proton-proton collisions is well studied, as is photon production.
- Binary scaling means to multiply yields in proton-proton by the ratio of incident parton flux of a gold-gold collision to the analogous flux for proton-proton.
- This scaling basically works for high-energy photons ($2\,\mathrm{GeV}/c < p_T < 14\,\mathrm{GeV}/c$) (Adler 2005[4]).
- It doesn’t work for high p_T hadrons: at mid-rapidity,

$$R_{AA} \equiv \frac{dN(\text{gold-gold})/dp_T d\eta}{\langle N_{\text{binary}}\rangle dN(\text{proton-proton})/dp_T d\eta} \approx 0.2 \tag{1}$$

where $\langle N_{\text{binary}}\rangle$ is the number of nucleon-nucleon collisions in a “factorized” gold-gold collision.

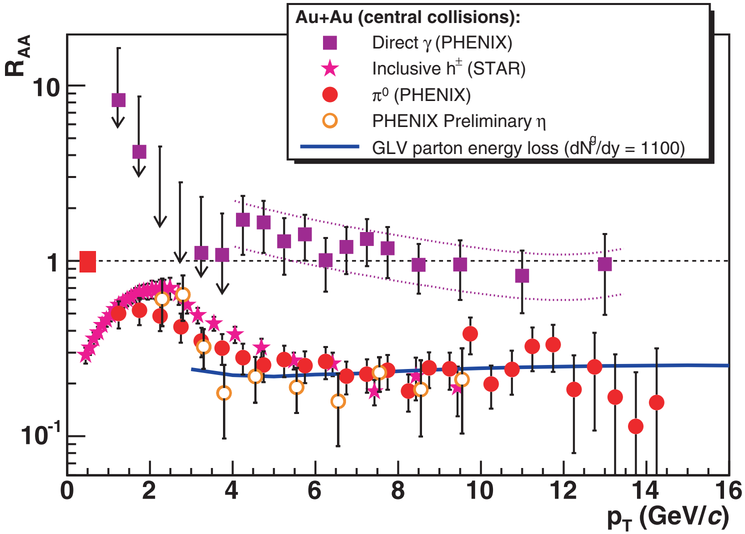

Figure 4: *Nuclear modification factor R_{AA} for photons and hadrons in 0 to 10% central gold-gold collisions.*

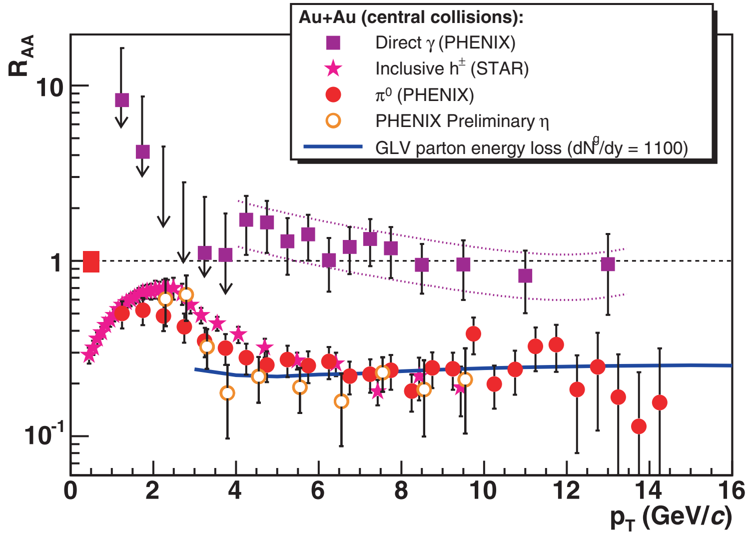

Figure 4: *Nuclear modification factor R_{AA} for photons and hadrons in 0 to 10% central gold-gold collisions.*

Can AdS/CFT explain this deficit?

The entropy and viscosity calculations have drawn the attention of RHIC phenomenologists, as well as DOE higher-ups:

> "The possibility of a connection between string theory and RHIC collisions is unexpected and exhilarating." — Ray Orbach, DOE Office of Science Director [5]

But before we proceed, some cautionary statements are worth noting — $\mathcal{N} = 4$ gauge theory misses several essential features of QCD:

- No confinement. Coupling doesn't run: it's a parameter you can dial.

  But is this so bad? We want to use AdS/CFT at finite temperature to model the QGP above T_c*. Phenomenological studies of RHIC physics routinely set* $v_s = 1/\sqrt{3}$ *and* $\epsilon \sim 1/t^{4/3}$ *(both corresponding to conformal invariance) for the QGP, e.g. when the energy density* ϵ *is significantly above* $1\,\mathrm{GeV}$*.*

- No chiral condensate.

  But is this so bad? The chiral condensate turns off around T_c *according to lattice calculations.*

- All fundamental matter fields are in adjoint representation: A_μ, four Majorana fermions λ_i, six real scalars X_I.

  This looks kind of bad. Maybe gauge interactions dominate the dynamics anyway?

3. Jet Quenching in AdS/CFT

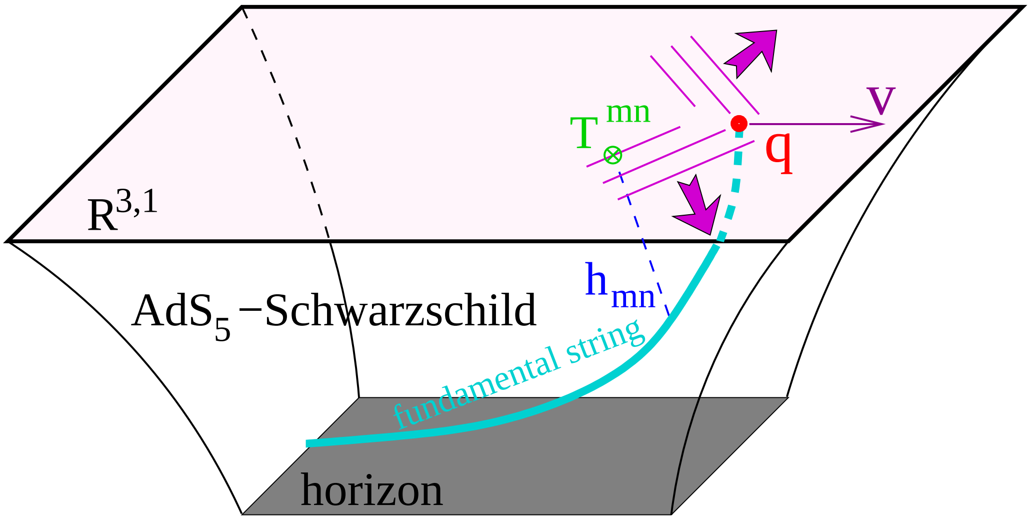

Figure 5: *In blue: the trailing string of an external quark (Herzog et al, 2006 [6]; Gubser 2006[7]). The dashed line shows classical propagation of a graviton from the string to the boundary, where its behavior can be translated into the stress-energy tensor $\langle T_{mn} \rangle$ of the boundary gauge theory.*

An analog of jet-quenching in AdS/CFT should involve a colored probe that we drag through the QGP, preferably at relativistic speeds. Readiest at hand are external quarks: strings with one end on the boundary.

Our background metric is

$$ds^2 = \frac{L^2}{z_H^2 y^2}\left(-h dt^2 + d\vec{x}^2 + z_H^2 \frac{dy^2}{h}\right) \qquad \boxed{h \equiv 1 - y^4} \qquad z_H = \frac{1}{\pi T} \tag{2}$$

We're interested in non-zero quark masses, so consider splitting one D3-brane from the large stack and putting it at a height $y_* \geq 0$, and treat it in the test-brane approximation. (Alternatively, wrap a D7 on an $S^3 \subset S^5$, and have it fill three extended directions plus the interval $0 \leq y \leq y_*$.) Then a string with one endpoint at y_*, going straight down into the horizon has a mass

$$m_{\text{static}} = \frac{L^2}{2\pi\alpha'}\left(\frac{1}{z_*} - \frac{1}{z_H}\right) = \frac{\sqrt{g_{YM}^2 N}}{2} T \left(\frac{z_H}{z_*} - 1\right) \tag{3}$$

In the QGP, u, d, and s quarks are dominated by thermal mass, whereas electroweak contribution still dominates for c and b. We use

$$m_u = m_d = m_s = 300\mathrm{MeV} \qquad m_c = 1400\mathrm{MeV} \qquad m_b = 4800\mathrm{MeV} \tag{4}$$

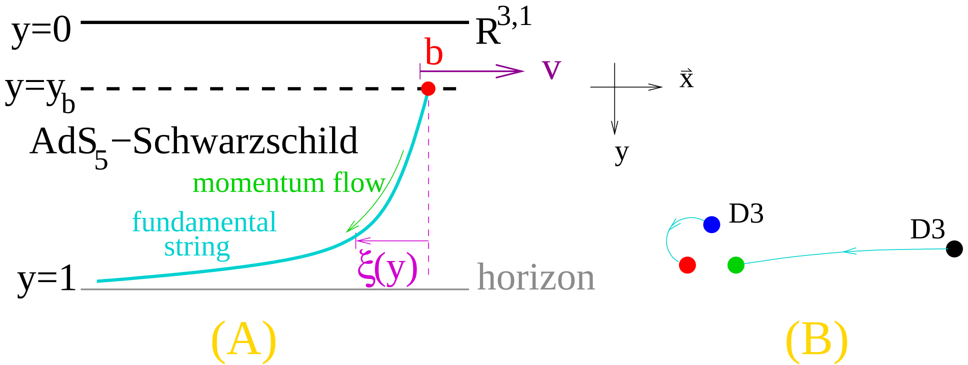

Figure 6: *(A) A finite mass quark moving at velocity* v *through the QGP can be represented as a string hanging from a "flavor brane" (Herzog et al, 2006). This picture is best justified for heavy quarks like* c *and* b*. In this figure and below, we use the radial coordinate* $y = z/z_H$*. (B) At* $T = 0$*, flavor branes can be realized by separating one D3-brane from several others. The massive* W *boson is similar to a heavy quark. We also show an* $R\bar{B}$ *gluon.*

3.1. A drag force computation

We need to know the shape of the trailing string and the momentum flow down it. We assume a "co-moving" ansatz, and parameterize the worldsheet as:

$$(t, x^1, x^2, x^3, y) = (\tau, vt + \xi(y), 0, 0, \sigma) \tag{5}$$

A "reduced" lagrangian follows from the Nambu-Goto action:

$$\mathcal{L} = -\frac{1}{y^2}\sqrt{1 + \frac{h\xi'^2}{z_H^2} - \frac{v^2}{h}} \tag{6}$$

And the solution is

$$\xi' = -\frac{v z_H y^2}{1 - y^4} \qquad \xi = -\frac{v z_H}{4i}\left(\log\frac{1-iy}{1+iy} + i\log\frac{1+y}{1-y}\right) . \tag{7}$$

This is deceptively real, since the argument for the first $\log$ is just a phase.

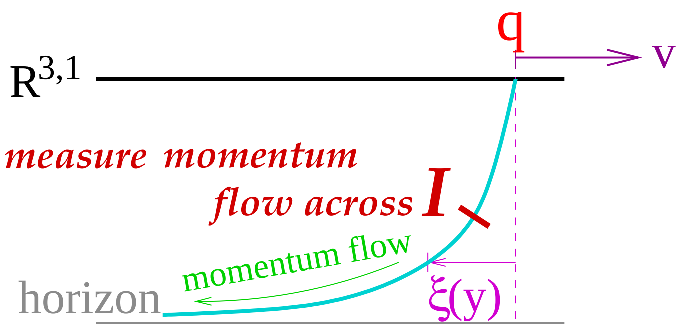

Figure 7: *The drag force is computed by measuring the momentum flux down the string. The position of $\mathcal{I}$ is arbitrary because the energy-momentum current is conserved.*

Momentum and energy drains down the string:

$$\Delta P_1 = -\int_{\mathcal{I}} dt\,\sqrt{-g}\,P^y{}_{x^1} = \frac{dp_1}{dt}\Delta t\,. \tag{8}$$

dp_1/dt is precisely the drag force:

$$F \equiv \frac{dp}{dt} = -\frac{\pi\sqrt{g_{YM}^2 N}T^2}{2}\frac{v}{\sqrt{1-v^2}}\,. \tag{9}$$

The expression for the string shape ξ holds for any mass (i.e., y_*) – just chop off the string above y_*. The drag force expression holds for heavy quarks, $m \gg T$, so that y_* is near the boundary, and we can use standard relativistic expressions like $E = \sqrt{p^2 + m^2}$ and $p = mv/\sqrt{1 - v^2}$.

$$F \equiv \frac{dp}{dt} = -\frac{\pi\sqrt{g_{YM}^2 N} T^2}{2} \frac{v}{\sqrt{1 - v^2}} \approx -\frac{\pi\sqrt{g_{YM}^2 N} T^2}{2m} p \,. \tag{10}$$

Simply integrate this to find

$$p(t) = p_0 e^{-t/t_0} \,, \qquad t_0 = \frac{2}{\pi\sqrt{g_{YM}^2 N}} \frac{m}{T^2} \,. \tag{11}$$

Plug in $T = 318\,\mathrm{MeV}$ and $\lambda = 10$, we find that $t_0 = 0.6\,\mathrm{fm/c}$ for charm, and $t_0 = 1.9\,\mathrm{fm/c}$ for bottom, compared to $t_{\mathrm{QGP}} \approx 6\,\mathrm{fm/c}$ for the typical lifetime of the QGP. This temperature is also a significant overestimate, convenient so that $z_H = 1/\pi T = 1\,\mathrm{GeV}^{-1}$. A more realistic temperature would reduce the quenching effect – QGP also cools substantially as it expands.

3.2. Graviton perturbations

A good measure of the energy loss is $\langle T_{mn} \rangle$ in the boundary gauge theory. Here we'll attempt a concise description of the calculation.

$\langle T_{mn} \rangle$ is determined by the behavior near the boundary of linearized graviton perturbations of AdS_5-Schwarzschild:

$$ds^2_{(0)} = G^{(0)}_{\mu\nu} dx^\mu dx^\nu = \frac{L^2}{z_H^2 y^2} \left(-h dt^2 + d\vec{x}^2 + z_H^2 \frac{dy^2}{h} \right) \qquad h \equiv 1 - y^4 \,. \quad (12)$$

$$G_{\mu\nu} = G^{(0)}_{\mu\nu} + h_{\mu\nu} \,, \quad (13)$$

The Einstein equations are

$$R^{\mu\nu} - \frac{1}{2} G^{\mu\nu} R - \frac{6}{L^2} G^{\mu\nu} = \tau^{\mu\nu} \,, \quad (14)$$

where $\tau^{\mu\nu}$ is the stress-energy of the trailing string.

A priori, this leaves us with 15 equations for 15 perturbative modes. The stress tensor involves delta functions at the location of the string, so move to Fourier space. This gives a series of coupled ordinary differential equations in y for the co-moving Fourier components $h_K^{\mu\nu}$. Then:

- Choose "axial gauge," $h_K^{\mu y} = 0$. Now there are 10 independent quantities h_K^{mn}, where $0 \leq m, n \leq 3$.

- We are left with 10 second order equations of motions, $\mathcal{E}^{mn} = 0$, and 5 first order constraints, $\mathcal{E}^{\mu y} = 0$.

- The differential equations may be partially decoupled and simplified by making a series of field redefinitions. They are still complicated—see below.

- Since hep-th/0607022, we have generalized by allowing the trailing string to end on a flavor brane at $y = y_*$. This is accomplished simply by including a factor of $\theta(y - y_*)$ in $\tau_{\mu\nu}$.

- We take $\vec{K} = (K_1, K_\perp, 0) = K(\cos\theta, \sin\theta, 0)$.

Here's the full problem:

$$h^K_{\mu\nu} = \frac{\kappa^2}{2\pi\alpha'}\frac{1}{\sqrt{1-v^2}}\frac{L}{z_H^2 y^2}\begin{pmatrix} H_{00} & H_{01} & H_{02} & H_{03} & 0 \\ H_{10} & H_{11} & H_{12} & H_{13} & 0 \\ H_{20} & H_{21} & H_{22} & H_{23} & 0 \\ H_{30} & H_{31} & H_{32} & H_{33} & 0 \\ 0 & 0 & 0 & 0 & 0 \end{pmatrix}. \tag{15}$$

$$K = \sqrt{K_1^2 + K_\perp^2} \qquad \theta = \tan^{-1}\frac{K_\perp}{K_1} \tag{16}$$

$$A = \frac{-H_{11} + 2\cot\theta H_{12} - \cot^2\theta H_{22} + \csc^2\theta H_{33}}{2v^2} \tag{17}$$

$$\left[\partial_y^2 + \left(-\frac{3}{y} + \frac{h'}{h}\right)\partial_y + \frac{K^2}{h^2}(v^2\cos^2\theta - h)\right] A = \frac{y}{h} e^{-iK_1\xi/z_H}\vartheta(y - y_*) \tag{18}$$

$$B_1 = \frac{H_{03}}{K^2 v} \qquad B_2 = -\frac{H_{13} + \tan\theta H_{23}}{K^2 v^2} \tag{19}$$

$$\left[\partial_y^2 + \begin{pmatrix} -\frac{3}{y} & 0 \\ 0 & -\frac{3}{y} + \frac{h'}{h} \end{pmatrix}\partial_y + \frac{K^2}{h^2}\begin{pmatrix} -h & v^2\cos^2\theta h \\ -1 & v^2\cos^2\theta \end{pmatrix}\right]\begin{pmatrix} B_1 \\ B_2 \end{pmatrix} = \begin{pmatrix} 0 \\ 0 \end{pmatrix} \tag{20}$$

$$B_1' - hB_2' = 0 \tag{21}$$

$$C = \frac{-\sin\theta H_{13} + \cos\theta H_{23}}{K} \tag{22}$$

$$\left[\partial_y^2 + \left(-\frac{3}{y} + \frac{h'}{h}\right) + \frac{K^2}{h^2}(v^2\cos^2\theta - h)\right] C = 0 \tag{23}$$

$$D_1 = \frac{H_{01} - \cot\theta H_{02}}{2v} \qquad D_2 = \frac{-H_{11} + 2\cot 2\theta H_{12} + H_{22}}{2v^2} \tag{24}$$

$$\left[\partial_y^2 + \begin{pmatrix} -\frac{3}{y} & 0 \\ 0 & -\frac{3}{y} + \frac{h'}{h} \end{pmatrix}\partial_y + \frac{K^2}{h^2}\begin{pmatrix} -h & v^2\cos^2\theta h \\ -1 & v^2\cos^2\theta \end{pmatrix}\right]\begin{pmatrix} D_1 \\ D_2 \end{pmatrix} = \frac{y}{h} e^{-iK_1\xi/z_H}\vartheta(y - y_*)\begin{pmatrix} 1 \\ 1 \end{pmatrix} \tag{25}$$

$$D_1' - hD_2' = \frac{y^3}{ivK_1} e^{-iK_1\xi/z_H} \vartheta(y-y_*) \tag{26}$$

$$E_1 = \frac{1}{2}\left(-\frac{3}{h}H_{00} + H_{11} + H_{22} + H_{33}\right) \qquad E_2 = \frac{H_{01} + \tan\theta H_{02}}{2v}$$
$$E_3 = \frac{H_{11} + H_{22} + H_{33}}{2} \qquad E_4 = \frac{-H_{11} - H_{22} + 3\cos 2\theta(-H_{11} + H_{22}) + 2H_{33} - 6\sin 2\theta H_{12}}{4} \tag{27}$$

$$\begin{aligned}\Bigg[\partial_y^2 + &\begin{pmatrix} -\frac{3}{y} + \frac{3h'}{2h} & 0 & 0 & 0 \\ 0 & -\frac{3}{y} & 0 & 0 \\ 0 & 0 & -\frac{3}{y} + \frac{h'}{2h} & 0 \\ 0 & 0 & 0 & -\frac{3}{y} + \frac{h'}{h} \end{pmatrix} \partial_y \\ &+ \frac{K^2}{3h^2} \begin{pmatrix} -2h & 12v^2\cos^2\theta & 6v^2\cos^2\theta + 2h & 0 \\ 0 & 0 & 2h & h \\ 0 & 0 & -2h & -h \\ 2h & -12v^2\cos^2\theta & 0 & 3v^2\cos^2\theta + h \end{pmatrix}\Bigg] \begin{pmatrix} E_1 \\ E_2 \\ E_3 \\ E_4 \end{pmatrix} \\ &= \frac{y}{h} e^{-iK_1\xi/z_H} \vartheta(y-y_*) \begin{pmatrix} 1 + \frac{v^2}{h} \\ 1 \\ -1 + v^2 - \frac{v^2}{h} \\ v^2\,\frac{1+3\cos 2\theta}{2} \end{pmatrix}\end{aligned} \tag{28}$$

$$\begin{aligned}\Bigg[&\begin{pmatrix} 0 & 1 & 1 & 0 \\ -h & 0 & -3v^2\cos^2\theta - h & -h \\ h & 0 & 2 & 0 \end{pmatrix} \partial_y \\ &+ \frac{1}{6h} \begin{pmatrix} 0 & -6h' & -3h' & 0 \\ -3hh' & 18v^2\cos^2\theta h' & 3(3v^2\cos^2\theta + h)h' & 0 \\ 2K^2yh & -12K^2v^2y\cos^2\theta & -2K^2y(3v^2\cos^2\theta - h) & 2K^2yh \end{pmatrix}\Bigg] \begin{pmatrix} E_1 \\ E_2 \\ E_3 \\ E_4 \end{pmatrix} \\ &= \frac{h'}{4Kyh} e^{-iK_1\xi/z_H} \vartheta(y-y_*) \begin{pmatrix} -ivy\sec\theta \\ 3ivy\cos\theta(v^2+h) \\ K(v^2-h) \end{pmatrix} .\end{aligned} \tag{29}$$

To solve the 10 second order equations of motion for specified K, we must fix 20 integration constants.

- Think of 15 as being fixed at the boundary of AdS_5-Schwarzschild (that is, $y = 0$) and the remaining 5 at the horizon to suppress solutions describing gravitons coming *out* of the black hole. Each set of equations has exactly one non-vanishing oscillatory mode at the horizon whose frequency must have the correct sign.

- Of the 15 boundary conditions at $y = 0$, five come from imposing the first-order constraints. This is arbitrary: the constraints can be imposed anywhere.

- The 10 remaining boundary conditions come from requiring $H_{\mu\nu} \to 0$ as $y \to 0$, i.e., the metric in the boundary theory remains Minkowski.

In practice, to proceed we:

- Note that the B and C sets are odd under the Z_2 reflection in the (x_1, x_2) plane spanned two comoving momenta, so these functions must be zero.
- For the seven functions A, D, and E, find solutions to the equations of motion that are asymptotically exact at the boundary and horizon. Near the boundary, each mode roughly takes the form $H \sim P + Qy^4$
- Pick some specific $\vec{K} = (K_1, K_\perp)$.
- Set A for each mode to zero at the boundary (n integration constants in each set with n equations).
- Impose the constraint equations at the boundary, which relate the $Q's$ in each set – there are $n - 1$ first-order constraints per set. We're left with one remaining integration constant Q per set – call them Q_A, Q_D, Q_E.
- Adjust Q_X until the one undesirable outgoing mode at the horizon goes away.

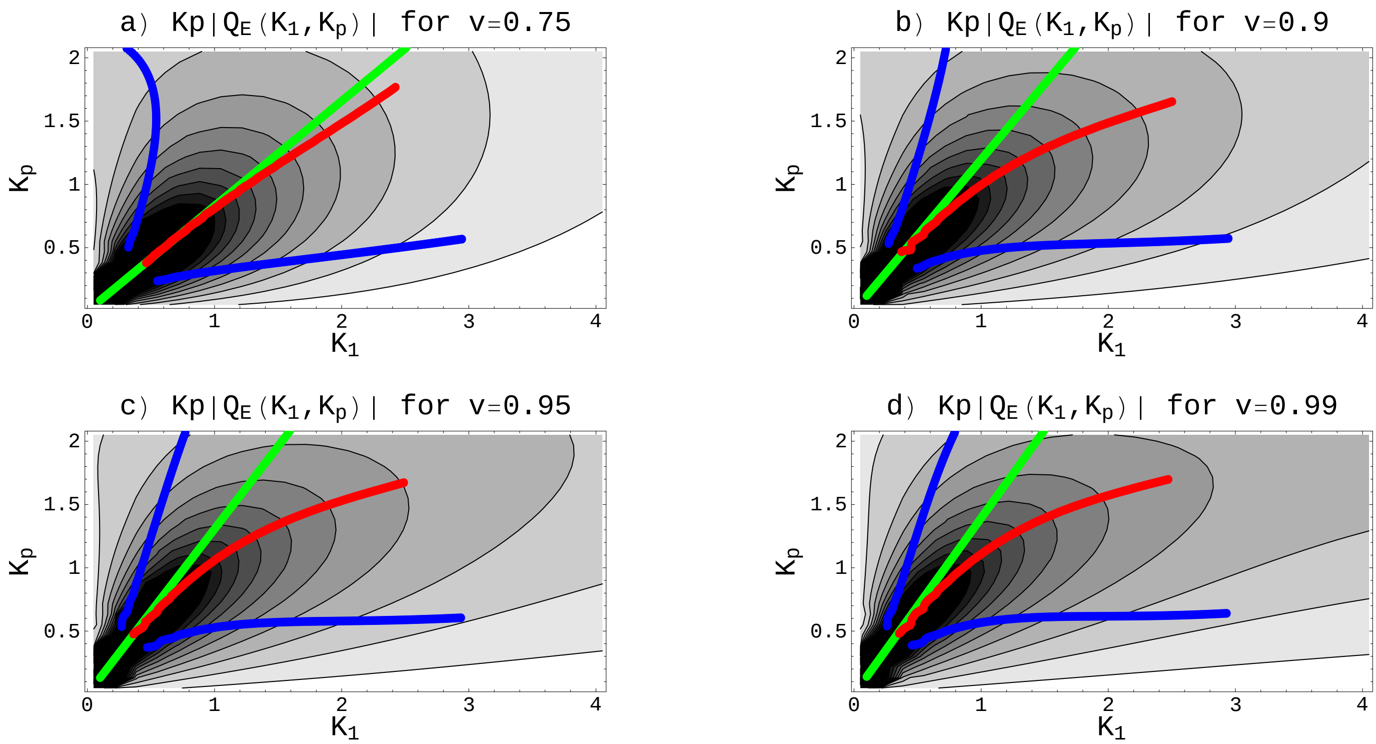

Figure 8: *Contour plots of* $K_\perp|Q_E^K|$ *for various values of* v. Q_E^K *is proportional to the* K*-th Fourier component of the energy density after a near-field subtraction. The phase space factor* $K_\perp$ *arises in Fourier transforming back to position space. The green line shows the Mach angle. The red curve shows where* $K_\perp|Q_E^K|$ *is maximized for fixed* $K = \sqrt{K_1^2 + K_\perp^2}$. *The blue curves show where* $K_\perp|Q_E^K|$ *takes on half its maximum value for fixed* K. *For* $T = 318\,\mathrm{MeV}$, *momenta axes are in units of* GeV.

Same plot as previous page in polar coordinates: $K_1 = K\cos\theta$, $K_\perp = K\sin\theta$

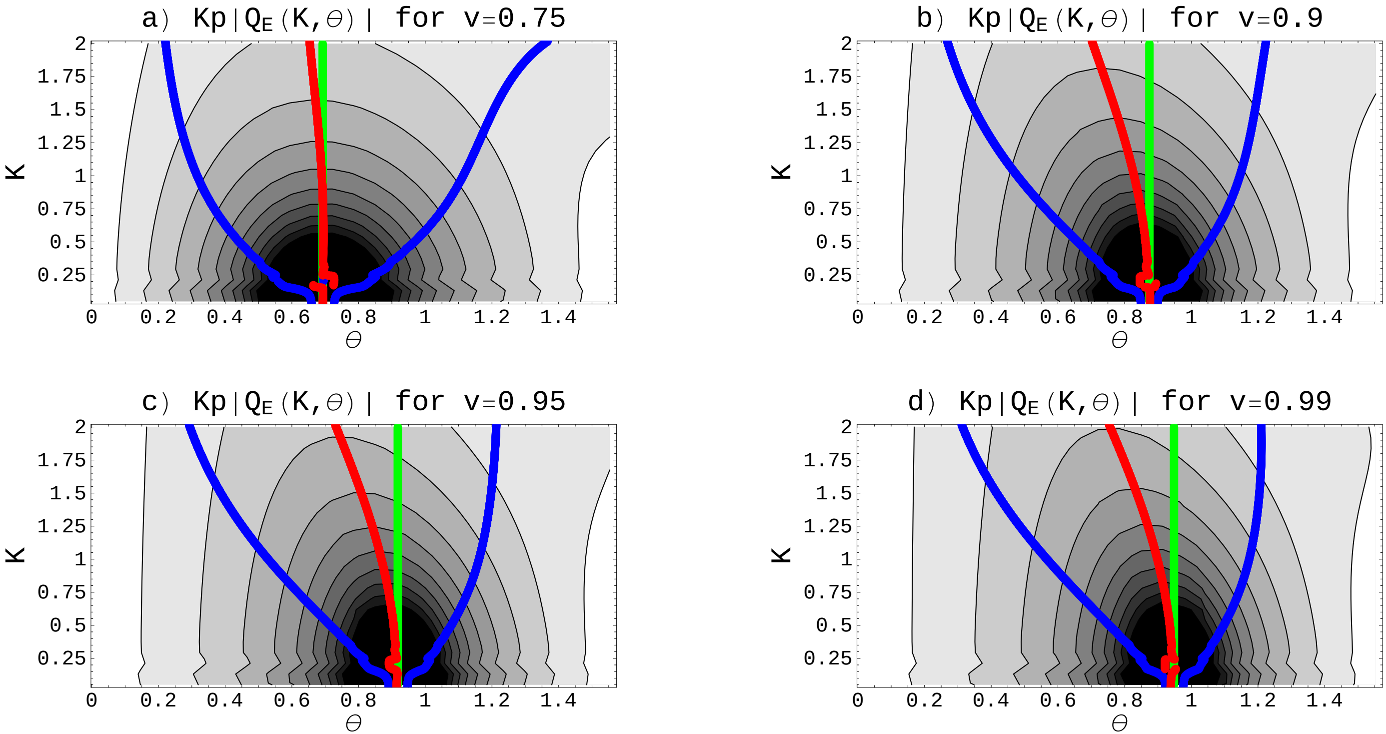

Energy density for a charm quark in polar coordinates, without a near-field subtraction – qualitatively identical to infinite mass case with the near-field subtraction

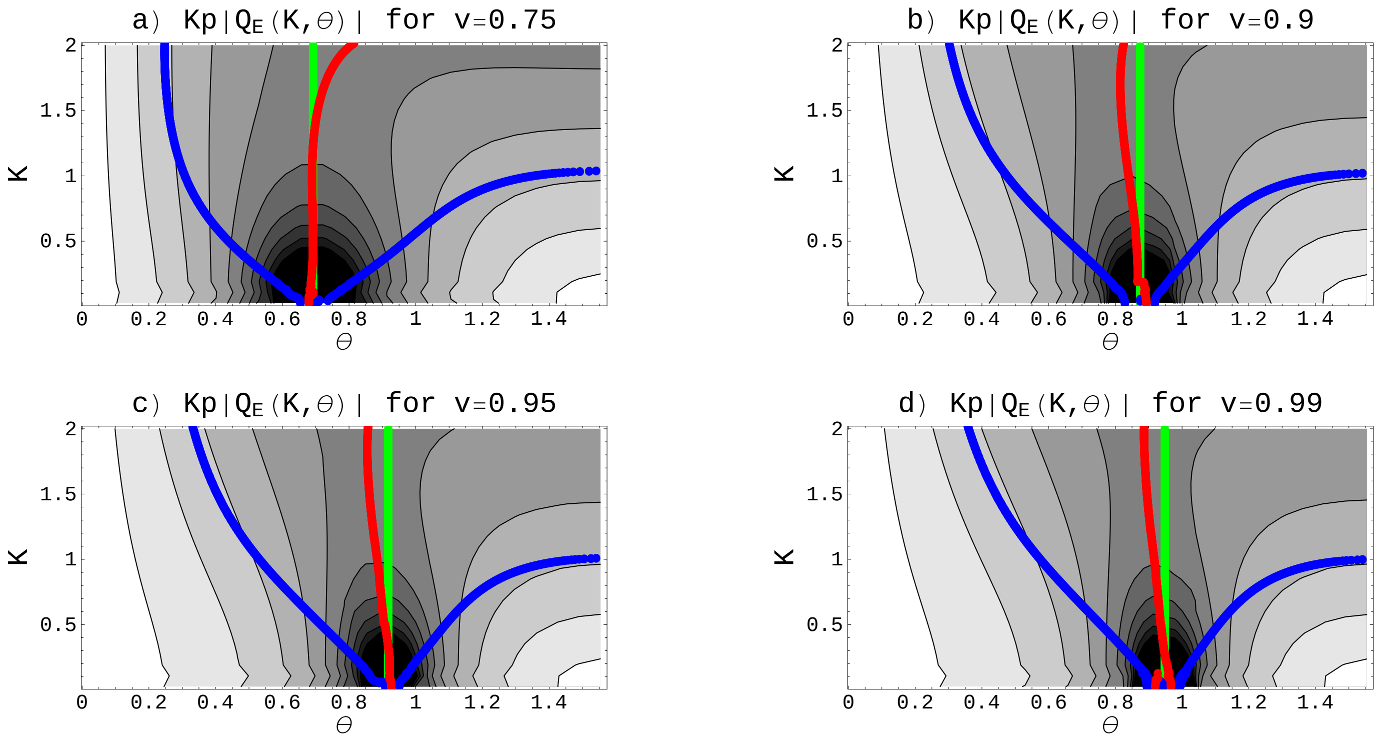

Figure 9: $K_\perp Q_E(K,\theta)$ *for* $y_* = 0.26$*, i.e.,* $m_c = 1400\mathrm{MeV}$, $T = 318\mathrm{MeV}$*, and* $\lambda = 10$

3.3. The wake of a quark

A much-discussed aspect of RHIC's current experimental program hinges on the following picture:

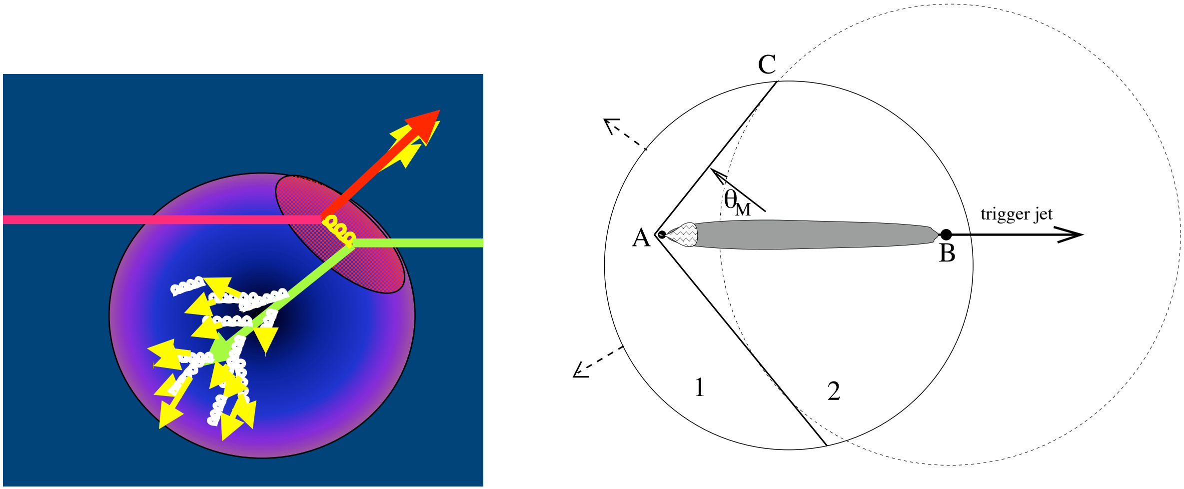

Figure 10: *Left: A di-jet event with significant away-side jet quenching. (Jacak [8]). Right: The away-side parton may generate a sonic boom, with* $\theta_M = \cos^{-1}(c_s/v)$ *the Mach angle. From (Casalderrey-Solana et al, 2004 [9]).*

- Two hard partons collide near the surface of the QGP.
- One escapes and fragments into the "near side" jet.
- The other plows through the QGP and dissipates a lot of energy.

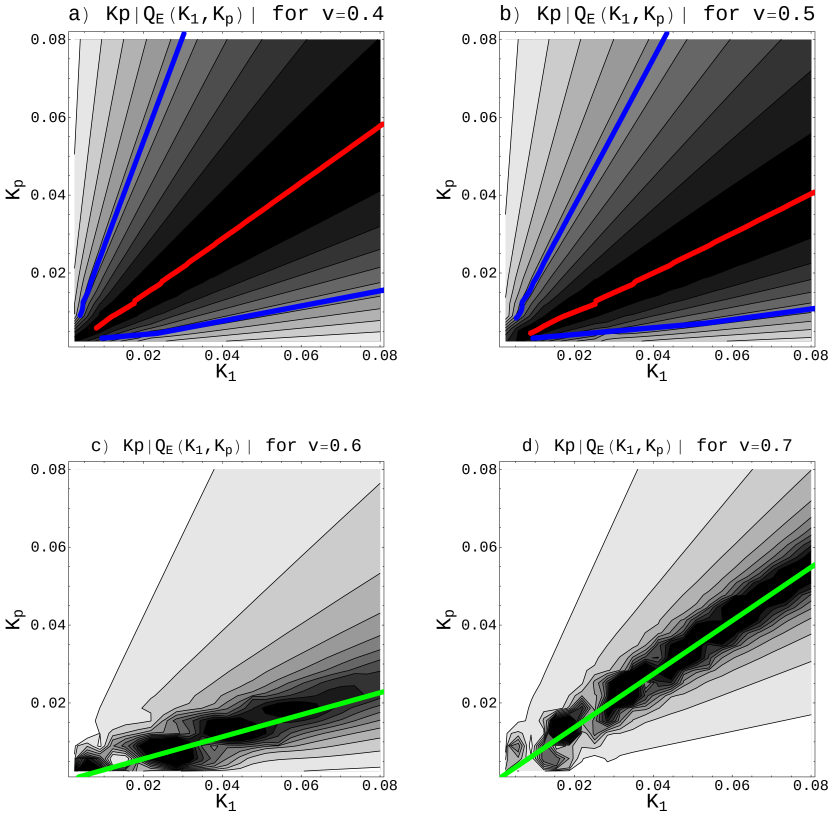

Figure 11: *Numerical data for stress tensor at low K for various velocities. Speed of sound is $c_s = 1/\sqrt{3} \approx 0.577$. Green lines indicate the Mach angle, as usual. Red lines are peak of distributions, and blue lines are locations of the half-maximum.*

The sonic boom can also be immediately identified in the graviton calculation via a small K expansion for the stress tensor, which can be found by matching boundary and horizon asymptotic solutions that are K-exact to small K solutions for all y.

$$\langle T_{00}^K \rangle \propto \frac{3iv(1+v^2)\cos\theta}{2K\left(1-3v^2\cos^2\theta\right)} - \frac{3v^2\cos^2\theta\left[2+v^2\left(1-3\cos^2\theta\right)\right]}{2\left(1-3v^2\cos^2\theta\right)^2} + O(K)$$

$$= \frac{3iv(1+v^2)\cos\theta}{2K} \frac{1}{\left(1-3v^2\cos^2\theta\right)\left(1-\frac{ivK\cos\theta}{1+v^2}\right) - ivK\cos\theta} + O(K)\,. \tag{30}$$

First expression is clearly singular at each order in K at the angle given by $\cos\theta = \frac{1}{v\sqrt{3}}$, which is the Mach angle. Second expression is equal, up to $O(K)$ terms, but it is regular and sharply peaked at the Mach angle, and appears to be a better fit to the numerics.

The sonic boom picture and related theoretical proposals suggest that high-angle emission carries away a lot of the energy. And data seems to confirm this:

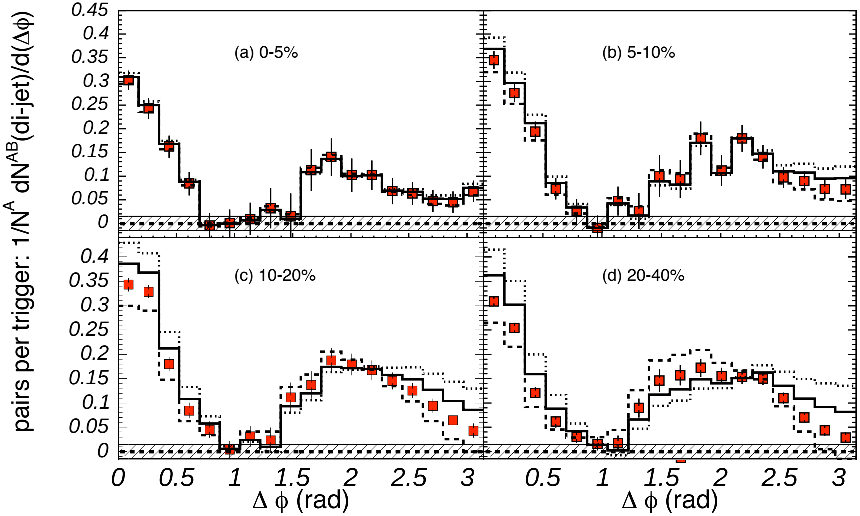

Figure 12: *Histograms of the azimuthal angle between the trigger hadron (with* $2.5\,\mathrm{GeV}/c < p_T < 4\,\mathrm{GeV}/c$*) and the partner hadron (with* $1\,\mathrm{GeV}/c < p_T < 2.5\,\mathrm{GeV}/c$*). Away-side jet splitting, illustrated by the broad peak around* $\Delta\phi = 2$*, is evidence for high-angle emission in the QGP. (Adler 2005 [10]).*

The numerical data from AdS/CFT agrees (at least) qualitatively with the RHIC data:

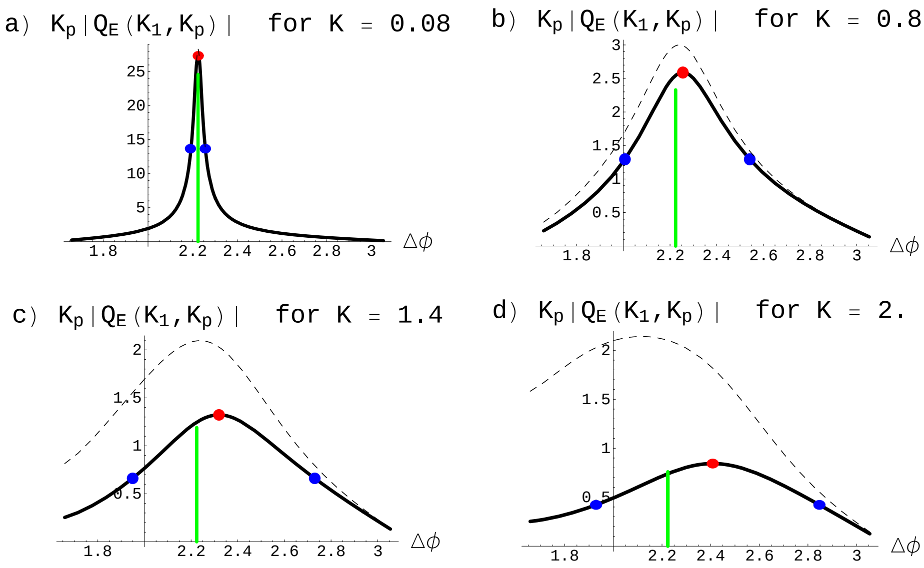

Figure 13: $K_\perp|Q_E^K|$ *at fixed* K *as a function of angle, for* $v = 0.95$. $\Delta\phi = \pi - \theta$ *where* $\theta = \tan^{-1} K_\perp/K_1$. *The dashed lines are from an analytic estimate, and the solid lines are from numerics. The green line is the Mach angle; the red dot is the peak; and the blue dots are at half the peak height. Plots (c) and (d) are in the ballpark of the experimental study summarized in the previous figure.* K *is the total momentum, in units of* GeV *if* $T = 318\,\mathrm{MeV}$.

4. Conclusions

- A simple type IIB string configuration helps elucidate the physics of jet quenching at RHIC.
- Broadly directional peaks agree qualitatively with observed splitting of the away-side jet.
- The string theory setup involves significant idealizations of the experimental setup, notably replacing QCD by $\mathcal{N} = 4$ super-Yang-Mills.
- Nevertheless, we hope that further improvements may lead to more precise comparisons of string theory predictions with data.

References

[1] The full MPEG can be found at http://www.bnl.gov/RHIC/images/movies/Au-Au_200GeV.mpeg, where it is attributed to the UrQMD group at Frankfurt, see http://www.physik.uni-frankfurt.de/ ∼urqmd/.

[2] M. Kaneta and N. Xu, "Centrality dependence of chemical freeze-out in Au + Au collisions at RHIC," `nucl-th/0405068`.

[3] F. Karsch, "Lattice QCD at high temperature and density," *Lect. Notes Phys.* **583** (2002) 209–249, `hep-lat/0106019`.

[4] **PHENIX** Collaboration, S. S. Adler *et. al.*, "Centrality dependence of direct photon production in s(NN)**(1/2) = 200-GeV Au + Au collisions," *Phys. Rev. Lett.* **94** (2005) 232301, `nucl-ex/0503003`.

[5] http://www.bnl.gov/bnlweb/pubaf/pr/PR_display.asp?prID=05-38.

[6] C. P. Herzog, A. Karch, P. Kovtun, C. Kozcaz, and L. G. Yaffe, "Energy loss of a heavy quark moving through N = 4 supersymmetric Yang-Mills plasma," `hep-th/0605158`.

[7] S. S. Gubser, "Drag force in AdS/CFT," `hep-th/0605182`.

[8] Talk by B. Jacak, "Plasma physics of the quark gluon plasma", Boulder, May 2006. Available at http://www4.rcf.bnl.gov/∼steinber/boulder2006/.

[9] J. Casalderrey-Solana, E. V. Shuryak, and D. Teaney, "Conical flow induced by quenched QCD jets," *J. Phys. Conf. Ser.* **27** (2005) 22–31, `hep-ph/0411315`.

[10] **PHENIX** Collaboration, S. S. Adler *et. al.*, "Modifications to di-jet hadron pair correlations in Au + Au collisions at s(NN)**(1/2) = 200-GeV," `nucl-ex/0507004`.